Basic Res Cardiol (2015) 110:456
DOI 10.1007/s00395-014-0456-3

ORIGINAL CONTRIBUTION

# Chronic $\beta_1$-adrenergic blockade enhances myocardial $\beta_3$-adrenergic coupling with nitric oxide-cGMP signaling in a canine model of chronic volume overload: new insight into mechanisms of cardiac benefit with selective $\beta_1$-blocker therapy

**Danielle M. Trappanese · Yuchuan Liu · Ryan C. McCormick · Alessandro Cannavo · Gayani Nanayakkara · Marina M. Baskharoun · Harish Jarrett · Felix J. Woitek · D. Michael Tillson · A. Ray Dillon · Fabio A. Recchia · Jean-Luc Balligand · Steven R. Houser · Walter J. Koch · Louis J. Dell'Italia · Emily J. Tsai**

Received: 29 July 2014 / Revised: 21 November 2014 / Accepted: 28 November 2014 / Published online: 6 December 2014


**Abstract** The $\beta_1$-adrenergic antagonist metoprolol improves cardiac function in animals and patients with chronic heart failure, isolated mitral regurgitation (MR), and ischemic heart disease, though the molecular mechanisms remain incompletely understood. Metoprolol has been reported to upregulate cardiac expression of $\beta_3$-adrenergic receptors ($\beta_3$AR) in animal models. Myocardial $\beta_3$AR signaling via neuronal nitric oxide synthase (nNOS) activation has recently emerged as a cardioprotective pathway. We tested whether chronic $\beta_1$-adrenergic blockade with metoprolol enhances myocardial $\beta_3$AR coupling with nitric oxide-stimulated cyclic guanosine monophosphate ($\beta_3$AR/NO-cGMP) signaling in the MR-induced, volume-overloaded heart. We compared the expression, distribution, and inducible activation of $\beta_3$AR/NO-cGMP signaling proteins within myocardial membrane microdomains in dogs (canines) with surgically induced MR, those also treated with metoprolol succinate (MR+βB), and unoperated controls. $\beta_3$AR mRNA transcripts, normalized to housekeeping gene RPLP1, increased $4.4 \times 10^3$- and $3.2 \times 10^2$-fold in MR and MR+βB hearts, respectively, compared to Control. Cardiac $\beta_3$AR expression was increased 1.4- and nearly twofold in MR and MR+βB, respectively, compared to Control. $\beta_3$AR was detected within caveolae-enriched lipid rafts ($Cav3^+$LR) and heavy density, non-lipid raft membrane (NLR) across all groups. However, in vitro selective $\beta_3$AR stimulation with BRL37344 (BRL) triggered cGMP production within only NLR of MR+βB. BRL induced $Ser^{1412}$ phosphorylation of nNOS within NLR of MR+βB, but not Control or MR, consistent with detection of NLR-specific $\beta_3$AR/NO-cGMP coupling. Treatment with metoprolol prevented MR-associated oxidation of NO biosensor soluble guanylyl cyclase (sGC) within NLR. Metoprolol therapy also prevented MR-induced relocalization of sGC$\beta_1$ subunit away from

D. M. Trappanese and Y. Liu contributed equally.

D. M. Trappanese · Y. Liu · R. C. McCormick · G. Nanayakkara · M. M. Baskharoun · H. Jarrett · F. J. Woitek · F. A. Recchia · S. R. Houser · E. J. Tsai (✉)
Cardiovascular Research Center, Temple University School of Medicine, 3500 North Broad Street, MERB 1047, Philadelphia, PA 19140, USA
e-mail: emily.tsai@tuhs.temple.edu

A. Cannavo · W. J. Koch
Center for Translational Medicine, Temple University School of Medicine, Philadelphia, PA, USA

D. M. Tillson · A. R. Dillon
College of Veterinary Medicine, Auburn University, Auburn, AL, USA

F. A. Recchia · S. R. Houser · E. J. Tsai
Department of Physiology, Temple University School of Medicine, Philadelphia, PA, USA

F. A. Recchia
Institute of Life Sciences, Scuola Superiore Sant'Anna, Pisa, Italy

J.-L. Balligand
Institute of Experimental and Clinical Research, Catholic University of Louvain, Brussels, Belgium

L. J. Dell'Italia
Division of Cardiovascular Disease, Department of Medicine, University of Alabama, Birmingham, AL, USA

E. J. Tsai
Cardiology Section, Department of Medicine, Temple University School of Medicine, Philadelphia, PA, USA

caveolae, suggesting preserved NO-sGC-cGMP signaling, albeit without coupling to $\beta_3$AR, within MR+βB caveolae. Chronic $\beta_1$-blockade is associated with myocardial $\beta_3$AR/NO-cGMP coupling in a microdomain-specific fashion. Our canine study suggests that microdomain-targeted enhancement of myocardial $\beta_3$AR/NO-cGMP signaling may explain, in part, $\beta_1$-adrenergic antagonist-mediated preservation of cardiac function in the volume-overloaded heart.

**Keywords** β-Blockade · Nitric oxide · Cyclic guanosine monophosphate · Caveolae · $\beta_3$-Adrenoceptor · Soluble guanylyl cyclase · Volume overload

## Introduction

β-blockers (βBs) confer cardiac benefit in disease through multiple mechanisms [4, 6, 16, 19, 27, 31, 38, 53], though many remain incompletely understood. In addition to disrupting the chronic adrenergic toxicity underlying heart failure (HF), βBs improve β-adrenoceptor (βAR) function largely by reversing the downregulation of myocardial $\beta_1$- and $\beta_2$AR [18, 59] and by countering the upregulation of G protein-coupled receptor kinase 2 (GRK2) expression [21] otherwise induced by chronic sympathetic activation. Thus, chronic βB therapy recouples βAR and G protein activity and restores βAR responsiveness. While studies of the effect of βB on βAR signaling in the diseased heart focus predominantly on $\beta_1$- and $\beta_2$ARs, few have examined its effect on $\beta_3$AR. Myocardial $\beta_2$AR expression is reportedly increased in HF animal models and patients [8, 35] and, in limited studies, even more so with chronic βB therapy [51, 64]. Recently, $\beta_3$AR activation has been shown to induce nitric oxide (NO)-mediated cardioprotection in animal models of cardiac pressure overload, neurohormone-induced hypertrophy, myocardial ischemia/reperfusion injury, and acute myocardial infarction [1, 5, 14, 41, 60]. Chronic $\beta_1$-blockade ($\beta_1$B) might well amplify cardioprotective $\beta_3$AR signaling in the pathologically remodeled heart. Intriguing but little explored, such a mechanism would suggest novel approaches to enhancing innate cardioprotective signaling while assuring compatibility with current guideline-directed medical therapy.

βAR signaling regulates cardiac myocyte contractility and hypertrophic signaling and, under normal physiological conditions, is modulated by NO via both direct [i.e., soluble guanylyl cyclase (sGC) activation] and indirect actions (e.g. *S*-nitrosylation, tyrosine nitration). NO activation of sGC, with its subsequent production of cyclic guanosine monophosphate (cGMP), blunts $\beta_1$- and $\beta_2$AR-stimulated cardiac contractility [55]. *S*-nitrosylation of GRK2 (also known as β-adrenergic receptor kinase 1 or βARK1) inhibits the desensitization and downregulation of $\beta_1$- and $\beta_2$ARs [61]. Conversely, $\beta_2$- and $\beta_3$AR signaling can activate NO synthase (NOS), thereby coupling βAR signaling with NO signaling. Unlike $\beta_1$- and $\beta_2$ARs, $\beta_3$ARs are stimulated at high catecholamine levels and thus may contribute more significantly to βAR signaling in conditions of catecholamine excess such as HF and mitral regurgitation (MR) [17, 34]. In the healthy, non-failing heart, $\beta_3$AR activation inhibits cardiac myocyte contraction and induces cardiac myocyte relaxation [15]. However, the effect of $\beta_3$AR signaling on cardiac contractility remains incompletely understood, as both negative [40] and positive [7] inotropic effects have been demonstrated with $\beta_3$AR stimulation in diseased, failing hearts. Importantly, transgenic mice with cardiac-specific overexpression of human $\beta_3$AR show enhanced cardiac contractility [26] and attenuated neurohormone-induced hypertrophic remodeling [5].

Gene expression analysis of left ventricular (LV) tissue recently revealed that cardiac βAR and NO signaling pathways are markedly altered in patients with isolated MR compared to control subjects [66]. Yet how the interaction between βAR and NO signaling differs in the stressed and pathologically remodeled heart is not fully understood. We previously demonstrated that NO-sGC-cGMP signaling is dysregulated in animal models of concentric and eccentric cardiac hypertrophy with respect to myocardial expression, subcellular localization, and oxidation of sGC heterodimer subunits [29, 57].

In prior studies, chronic $\beta_1$B therapy preserved normal cardiac myocyte contractility and enhanced βAR responsiveness in the experimental chronic MR canine model after four months of treatment [43]. In the present study, we used a 4-week chronic MR canine model to investigate the early effects of chronic $\beta_1$B therapy on myocardial NO-sGC-cGMP signaling as well as $\beta_3$AR/NO-cGMP coupling. We hypothesized that chronic $\beta_1$B therapy preserves normal NO-sGC-cGMP signaling and enhances myocardial $\beta_3$AR/NO-cGMP coupling in a microdomain-specific fashion, thereby potentially mediating later cardiac myocyte functional benefits. We focused on signaling within and outside of myocardial caveolae—small, flask-shaped, lipid- and protein-rich invaginations of the plasma membrane (PM) that compartmentalize signal transduction. Importantly, all three βAR subtypes [2, 30, 45, 47, 49], eNOS [23], nNOS [9], sGC [57], and calcium channels [32, 33], reside within caveolae; some, exclusively.

## Methods

### Animal experiments

Mitral regurgitation (MR) was induced in conditioned mongrel dogs (19–26 kg) by rupturing a papillary chord

under fluoroscopy, as previously described [25, 29, 46]. Sixteen dogs underwent chordal rupture and ten unoperated dogs served as controls. At 24 h after MR induction, half of the MR dogs were started on metoprolol succinate 100 mg by mouth once daily (MR $n = 8$, MR+βB $n = 8$). Two-dimensional and M-mode echocardiography (2.25-MHz transducer, ATL Ultramark VI) was performed at baseline and at the time of euthanasia (4 weeks after MR induction). Animals were maintained at a deep plane of general anesthesia using isoflurane and were mechanically ventilated. At the end of the in vivo experiments, the heart was arrested with intracardiac injection of KCl and quickly extirpated and placed in phosphate-buffered ice slush. The coronaries were flushed with oxygenated Krebs solution. A portion of the LV was cut and snap-frozen in liquid nitrogen for subsequent studies. We chose to study 4-week duration of therapy so as to identify early signaling changes that precede and thus underlie subsequent functional benefits already demonstrated with longer term treatment. Animal studies were approved by the Animal Services Committees at the University of Alabama at Birmingham and College of Veterinary Medicine, Auburn University and the Institutional Animal Care and Use Committee of Temple University School of Medicine. All animal protocols conformed to the Guide for the Care and Use of Laboratory Animals published by the National Institutes of Health (NIH publication No.85-23, revised 1996).

### Quantitative reverse transcription polymerase chain reaction (qRT-PCR)

Total RNA was extracted from flash-frozen LV myocardium using a spin column chromatography method (Animal Tissue RNA Purification Kit, Norgen Biotek, Ontario, Canada), according to the manufacturer's instructions. Reverse transcription (RT) was performed using the SuperScript III First-Strand Synthesis System (Invitrogen, Life Technologies) and oligo-dt primers according to the manufacturer's instructions. Real-time PCR (qPCR) was performed using QuantiFast SYBR® Green PCR Kit (Qiagen). Data were normalized to large ribosomal protein P1 (RPLP1) RNA expression. The following primer sets were used (forward, reverse): $\beta_3$AR (5′-CGCCTCCAACATACCCTACG-3′, 5′-CGCGTAGCCACGAGGAAAA-3′); RPLP1 (proprietary primer sequences, Qiagen). Individual samples were run in triplicate.

### Isolation of caveolin-3-enriched lipid raft fraction by isopycnic ultracentrifugation

Caveolae-enriched lipid raft fractions ($Cav3^+$LR) were prepared from snap-frozen LV tissue, using a discontinuous 35–5 % sucrose density gradient ultracentrifugation method as previously described [29, 57]. LV tissue homogenization was carried out on ice, in detergent-free buffer (50 mmol/L Tris–HCl, pH 7.6, 1 mmol/L EDTA, 1 mmol/L DTT, 2 mmol/L PMSF, 50 mmol/L NaF, 1 mmol/L Na Vanadate) with protease inhibitors (Mammalian Cocktail, Sigma-Aldrich). Following 1-h incubation on ice with intermittent vortex, 0.6 mL of tissue homogenate was mixed with 1.4 mL of 60 % (w/w) sucrose in 20 mmol/L KCl, 0.5 mmol/L $MgCl_2$ and placed at the bottom of an ultracentrifuge tube. A discontinuous 35–5 % sucrose gradient was formed by overlaying each sample with 1.3 mL of 35 % sucrose and then with 1.3 mL of 5 % sucrose. The sucrose density gradient was topped off with 0.5 mL of 200 mmol/L KCl. Each sample was then centrifuged at >180,000*g* for 16–18 h at 4 °C in a swinging bucket rotor (Beckman Instruments, Palo Alto, CA) without any brake. The top KCl layer was discarded and fractions were collected every 400 µl from the top sucrose layer corresponding to F1 (top, most buoyant) to F11 (bottom, least buoyant/heaviest).

A light-scattering band confined to the 35–5 % sucrose interface, typically F3–F5, corresponds to $Cav3^+$LR fractions. Ponceau staining and protein concentrations determined by bicinchoninic acid (BCA) assay confirmed that total protein distribution was weighted toward heavier sucrose density gradient fractions (F7 through F11) lacking caveolin-3 (Cav3) in all hearts. Proteins were precipitated using 0.1 % w/v deoxycholic acid in 100 % w/v trichloroacetic acid. Protein concentrations were determined by BCA protein assay (Pierce). Non-lipid raft (NLR, F11) and $Cav3^+$LR fractions (F3–F5) without TCA precipitation were also collected for BCA and subsequent cGMP assays. $Cav3^+$LR fractions were selected based upon greatest enrichment of Cav3 as detected by Western.

### Cardiomyocyte caveolae-immunoaffinity isolation

Cardiomyocyte caveolae organelles were isolated using a immunoaffinity protocol [42]. In brief, sheep anti-mouse IgG-coated magnetic beads (Dynabeads, Life Technologies, Carlsbad, CA) were pre-incubated with a monoclonal antibody specific for caveolin-3 (BD transduction) for 2 h at room temperature. Control beads were pre-incubated in PBS only. Both anti-Cav3 Dynabeads and control IgG Dynabeads were subsequently washed with PBS for 1 h at 4 °C on a rotator.

Plasmalemmal membrane rafts were fractionated from ventricular myocardial tissue as previously reported [44]. Canine LV (100 mg) was dounce homogenized in 1 mL ice cold, detergent-free Tricine buffer (20 mM Tricine, 1 mM EDTA, 250 mM sucrose, pH 7.4) and centrifuged at 1,000*g* for 10 min at 4 °C. Cell pellets were resuspended in 1 mL Tricine buffer, dounce homogenized, and centrifuged

again at 1,000*g* for 10 min at 4 °C. An aliquot of pooled supernatant (30 µl) was set aside as the homogenate (H) sample. The pooled supernatant was then mixed with 30 % Percoll (Sigma) in Tricine buffer and subjected to ultracentrifugation at >116,000*g* for 30 min at 4 °C (Beckman MLS50 rotor, 33,000 rpm, no break). The separated PM was collected, mixed with ice-cold MBS buffer (20 mM 2 N-morpholinoethane-sulfonic acid, 20 mM KCl, 135 mM NaCl), and microcentrifuged at approximately 21,000*g* for 30 min at 4 °C to pellet the membrane. The supernatant was discarded. The membrane pellet was resuspended in ice cold 1 mL PBS and sonicated on ice (30 s bursts × 3). An aliquot (30 µl) was set aside as the PM for subsequent Western blotting.

Remaining PM was incubated with the anti-Cav3-coated Dynabeads for 1 h at 4 °C, using a rotator. Bound material (B), representative of cardiomyocyte caveolae vesicles, was separated magnetically from unbound (U), non-caveolae membranes. An aliquot (30 µl) of the unbound fraction (U) was set aside for subsequent Western blotting. Using the magnetic rack, beads were washed five times with PBS, resuspended in 2× loading buffer (100 mM Tris, pH 6.8, 2 % SDS, 0.02 % bromophenol blue, 20 % glycerol, 100 mM DTT), and boiled at 95 °C for 5 min to dissociate the protein from the beads. Homogenate (H), PM, bound material representative of cardiomyocyte caveolae (B), and unbound material representative of non-caveolae plasmalemmal membrane (U) were subjected to SDS-PAGE and immunoblotted using the indicated antibodies.

### Western analysis

Protein extracts were run on SDS-PAGE gels, transferred to nitrocellulose membranes, and immunoblotted using primary antibody probes as follows: $\beta_3$AR (1:1,000, Abnova); sGC$\alpha_1$ (1:1,000, Abcam); sGC$\beta_1$ (1:4,000, Cayman Chemicals); Cav3 (1:10,000, BD Transduction); total nNOS (1:1,000, BD Transduction); phospho-nNOS (*Ser*$^{1412}$ p-nNOS, 1:1,000, gifted by K.J. Hurt, University of Colorado) [20]; GAPDH (1:10,000, cell signaling). Specificity of anti-sGC$\alpha_1$ and -$\beta_1$ antibodies was confirmed using protein extracts from sGC$\alpha_1^{-/-}$ and sGC$\beta_1^{-/-}$ mouse hearts as previously published [57]. Primary antibody binding was visualized by either horseradish peroxidase-conjugated secondary antibodies with enhanced chemiluminescence (GE Healthcare) or Alexa Fluor 680 or 800-conjugated secondary antibodies (molecular probes) with an Odyssey infrared imager (LI-COR). Densitometry analysis of immunoblots was performed using Image J Software (NIH) or Image Studio Software (Odyssey CLx v2.1, LI-COR).

### sGC activity assay and redox state determination

Baseline and agonist-stimulated cGMP levels of total LV, Cav3$^+$LR, and NLR from Control, MR, and MR+βB hearts were measured by direct cGMP ELISA kit (New East Biosciences, Malvern, PA), as previously described [29, 57]. LV homogenates, Cav3$^+$LR and NLR membrane fractions were pre-incubated at room temperature for 15 min in a solution for final concentrations of Tris 50 mM, pH 7.6, IBMX (3-isobutyl-1-methylxanthine) 0.75 mmol/L, creatine phosphate 3.5 mmol/L, creatinine phosphokinase 1 unit, GTP 1 mmol/L, and $MgCl_2$ 3 mmol/L. Samples were then incubated with or without DEA/NO (1 µmol/L) or BAY 60-2770 (0.01 µmol/L) at 37 °C for 10 min and subjected to diethyl ether extraction. cGMP levels of ether-extracted samples were measured by EIA according to kit manufacturer protocol. BAY60 compound was provided by J-P Stasch (Bayer AG, Wuppertal, Germany).

### In vitro functional assays of $\beta_3$AR/NO-cGMP coupling

Selective $\beta_3$AR agonist BRL 37344 (BRL, 0.1 and 1.0 µmol/L, Tocris Bioscience) was used to assess $\beta_3$AR induction of NO-sGC-cGMP signaling. cGMP levels were measured as above.

### Statistical analysis

All values are expressed as mean ± SEM. Statistical analyses were performed using: two-way ANOVA when determining interaction of conditions or the source of variance; one-way ANOVA followed by Tukey or Holm–Sidak's multiple comparison test as appropriate; Brown-Forsythe test of variance, if relevant; and two-tailed paired, ratio paired, or one-tailed unpaired Student's *t* test, as appropriate. Statistical significance was defined as $P < 0.05$. GraphPad Prism 6.0 was used for statistical and graphical analysis.

## Results

### MR-induced early eccentric remodeling persists and normal LV function remains preserved following 4 weeks of metoprolol therapy

As expected, dogs developed increased LV chamber dilation and decreased LV wall thickness to end-diastolic dimension, by 4 weeks post-MR induction, irrespective of metoprolol therapy (Table 1). LV fractional shortening remained normal in Control, MR, and MR+βB hearts at 4 weeks.

**Table 1** LV structure and function assessed by echocardiography in canine chronic MR model

| | Control | MR | MR+βB |
|---|---|---|---|
| LVEDD (cm) | 3.7 ± 0.1 | 4.5 ± 0.2* | 4.9 ± 0.2* |
| LVESD (cm) | 2.1 ± 0.1 | 2.5 ± 0.1* | 2.8 ± 0.1* |
| LVWT/LVEDD | 0.28 ± 0.03 | 0.19 ± 0.02* | 0.18 ± 0.01* |
| FS (%) | 43 ± 3 | 44 ± 3 | 43 ± 3 |

* $P < 0.05$ vs. control on two-tailed, unpaired Student's $t$ test

### Chronic metoprolol therapy increases myocardial $\beta_3$AR expression without altering membrane microdomain distribution

Although expressed at low levels in the normal adult heart, $\beta_3$AR is upregulated in the concentric hypertrophied and failing heart [8, 35, 60, 65]. We induced early stage eccentric hypertrophy via MR-mediated chronic volume overload in dogs, as previously described [29], treated some MR dogs with $\beta_1$B metoprolol succinate (MR+βB), and measured $\beta_3$AR mRNA and protein expression as well as $\beta_3$AR membrane microdomain distribution, comparing control, MR, and MR+βB animals. $\beta_3$AR mRNA expression, normalized to housekeeping gene RPLP1, increased $4.4 \times 10^3$- and $3.2 \times 10^2$-fold in MR and MR+βB, respectively, relative to control (Fig. 1a). We detected $\beta_3$AR by Western immunoblot at its predicted molecular weight of 43 kDa in both isolated adult canine cardiac myocytes and canine LV myocardium (Fig. 1b). Sensitivity and specificity of our $\beta_3$AR antibody was demonstrated by immunoblotting various tissue and fractions known to have differential $\beta_3$AR expression. As expected, $\beta_3$AR expression was enriched in the PM fraction of murine LV relative to LV total protein. Our immunoblot likewise confirmed greater hepatic than myocardial $\beta_3$AR expression [62]. $\beta_3$AR expression was also greater in LV of human $\beta_3$AR expressing transgenic mice than of wild type mice [5]. Chronic $\beta_1$AR-blockade potentiated the increase in myocardial $\beta_3$AR expression in MR, with 1.4 ± 0.1-fold and 1.9 ± 0.2-fold higher expression in MR and MR+βB, respectively, than in Control (Fig. 1c, d). We also examined the distribution of $\beta_3$AR in myocardial membrane microdomains as resolved by isopycnic ultracentrifugation. $\beta_3$AR was detected within caveolae microdomains ($Cav3^+$LR, F4–F5) and heavy density, non-lipid raft membrane fractions (NLR, F11) of all hearts (Fig. 1e). While overall expression varied amongst the study groups, distribution of $\beta_3$AR across myocardial membrane fractions was similar (Fig. 1f). Caveolae localization of $\beta_3$AR within cardiomyocytes was further verified by plasmalemmal caveolae-immunoaffinity isolation and immunoblot analysis (Fig. 1g). Since only myocytes exclusively express Cav3, caveolae-immunoaffinity isolation using anti-Cav3-antibody-coated magnetic beads ensured selection of only myocyte caveolae, and not that of endothelial cells, fibrocytes, or adipocytes.

### Selective $\beta_3$AR stimulation with BRL37344 (BRL) increases cGMP production within heavy density, NLR fractions

To assess $\beta_3$AR/NO-cGMP coupling within membrane microdomains, we measured cGMP levels within $Cav3^+$LR and NLR fractions at baseline and in response to the selective $\beta_3$AR agonist BRL, all in the presence of non-selective phosphodiesterase inhibitor IBMX. While basal cGMP levels did not vary amongst Control, MR, and MR+βB within respective membrane microdomains, basal cGMP levels within $Cav3^+$LR exceeded that within corresponding NLR of Control and MR+βB hearts (Fig. 2a). $\beta_3$AR stimulation at increasing concentrations of BRL did not induce cGMP production within $Cav3^+$LR of any study group (data not shown). Conversely, BRL did induce significant cGMP production within NLR of only MR+βB (Table 2; Fig. 2b). To verify that NO-inducible sGC cyclase activity was intact in NLR of all groups and not solely MR+βB, NO-donor DEA/NO-induced cGMP responses are shown for comparison. Thus, coupling of $\beta_3$AR and NO-sGC-cGMP signaling was uniquely detected in NLR of MR+βB.

### $\beta_3$AR couples with NO-sGC-cGMP signaling via nNOS activation

$\beta_3$AR stimulation has been demonstrated to modulate the phosphorylation and activity of NOS isoforms [1, 5, 41, 60]. While eNOS activation by $\beta_3$AR is inconsistently reported amongst various animal and human models [1, 40, 41, 60], recent in vitro studies of isolated neonatal rat ventricular cardiac myocytes and in vivo mouse studies demonstrated cardioprotective $\beta_3$AR signaling mediated via nNOS activation, specifically through $Ser^{1412}$ phosphorylation of nNOS [5, 41, 60]. To corroborate the role of this mechanism in BRL-induced cGMP production within MR+βB NLR, we assessed $Ser^{1412}$ p-nNOS and total nNOS by Western blot in BRL-stimulated NLR of Control, MR, and MR+βB hearts (Fig. 3a). Increased phosphorylation of nNOS upon BRL stimulation was detected in NLR of MR+βB but not MR or Control (Fig. 3b). These results are consistent with $\beta_3$AR/NO-cGMP coupling in the NLR domain in a $\beta_1$B therapy-dependent manner.

### Effect of $\beta_1$AR-blockade on myocardial membrane microdomain distribution of sGC subunits

As we have previously shown, $\alpha_1$ and $\beta_1$ subunits of the sGC heterodimer localize to both $Cav3^+$LR and NLR but

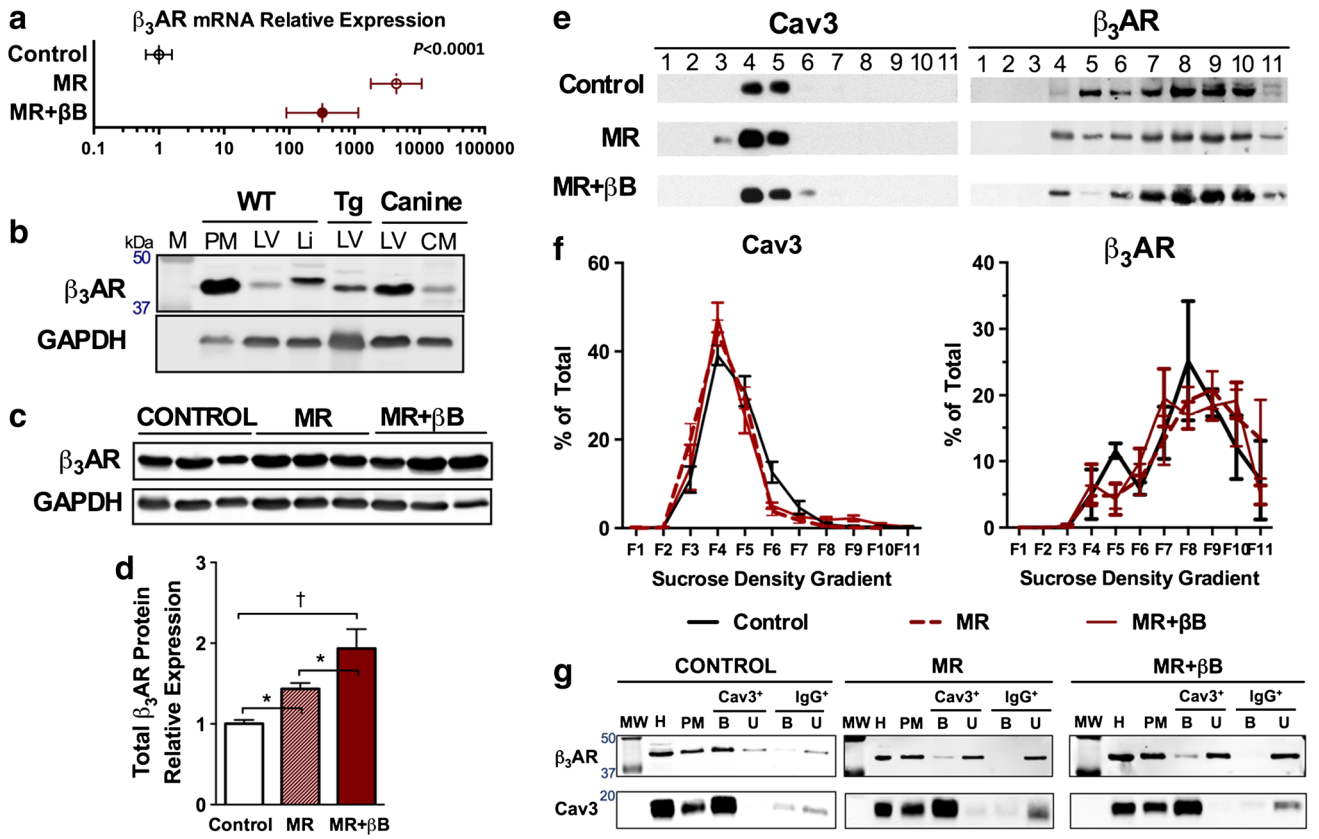


**Fig. 1** Volume-overload-induced $\beta_3$AR expression is potentiated by chronic $\beta_1$AR-blockade. **a** LV $\beta_3$AR mRNA levels normalized to RPLP1 mRNA levels (mean ± SEM) were determined in Control, MR, and MR+βB. $n = 5$ animals per group; one-way ANOVA $P < 0.0001$) **b** Western of $\beta_3$AR in LV plasma membrane fraction (PM) and total protein from myocardium (LV), isolated cardiac myocytes (CM), and liver (Li) of C57Bl/6 mice (WT), human $\beta_3$AR-expressing transgenic mice (Tg), and dogs. **c** Representative Westerns of $\beta_3$AR in LV total protein extracts from study dogs. **d** Summary densitometry analysis of total $\beta_3$AR expression normalized to GAPDH and Control levels. $n = 4$–6 animals per study group. one-way ANOVA $P = 0.002$. $^{*}P < 0.05$, $^{\dagger}P < 0.01$ on Holm–Sidak's multiple comparison test. **e** Representative Westerns of Cav3 and $\beta_3$AR across sucrose density gradient fractions (F1–F11) of Control, MR, and MR+βB. **f** Cav3 and $\beta_3$AR distribution is presented for each fraction as a percentage of the sum signal across all fractions. For Cav3, $n = 4$–7 per study group. For $\beta_3$AR, $n = 3$–6 per study group. **g** Cardiac myocyte plasmalemmal caveolae organelles were immunoaffinity-purified with anti-Cav3. $\beta_3$AR was detected LV homogenate (H), LV plasmalemmal membrane fraction (PM), cardiomyocyte plasmalemmal caveolae (*B* bound fraction), and in LV plasmalemmal membrane depleted of caveolae (*U* unbound fraction)

differentially relocalize in the hemodynamically stressed heart. Under pressure- and volume-overload cardiac stress, sGC$\beta_1$ relocalizes away from Cav3$^{+}$LR [29, 57]. Here, the distribution of sGC$\alpha_1$ was unperturbed by either volume overload or chronic $\beta_1$AR-blockade at this 4 week time point (Fig. 4a). Interestingly, chronic $\beta_1$AR–blockade prevented the shift of sGC$\beta_1$ towards NLR that was otherwise observed in MR hearts. In MR+βB, Cav3$^{+}$LR localization of sGC$\beta_1$ was preserved and relocalization of sGC$\beta_1$ to heavy density, NLR was abated (Fig. 4b).

## Chronic $\beta_1$AR-blockade is associated with less oxidized and more reduced sGC

Given the observed membrane distribution of the sGC subunits and $\beta_3$AR, physical colocalization of these proteins alone would not explain the functional coupling of $\beta_3$AR and NO-sGC-cGMP signaling detected exclusively within NLR of MR+βB. We hypothesized that chronic $\beta_1$AR-blockade may have impacted the redox state of sGC within the various membrane microdomains. Dependent upon its ferrous heme moiety, inducible cyclase activity of the sGC heterodimer varies with its redox state. Oxidized sGC does not respond normally to NO. Heme-free sGC is unresponsive to NO stimulation. sGC activators (e.g. BAY60) can stimulate sGC cyclase activity independent of NO or heme; oxidized sGC has a relatively potentiated response to sGC activators [24]. Thus, differential cyclase response of sGC to BAY60 versus NO-donor DEA/NO can reveal its redox state [48]. We previously showed that while NLR-localized sGC becomes oxidized in the volume-overloaded heart, caveolae-localized sGC does not

[29]. We measured cGMP levels of LV total protein extracts, Cav3$^+$LR, and NLR at baseline and following stimulation with DEA/NO and BAY60, all in the presence of IBMX (Fig. 5). BAY60-induced cGMP production exceeded DEA/NO-induced cGMP production in MR and MR+βB, suggesting an overall predominance of oxidized sGC in the volume-overloaded heart. However, BAY60-induced cGMP production in MR+βB was similar to that in Control, both lower than in MR, suggesting that chronic $\beta_1$AR-blockade blunts oxidation of sGC in the volume-overloaded heart (Fig. 5a). Alternatively, differential cyclase activity could reflect differential expression of sGC. Immunoblots of sGC subunits confirmed that sGC$\beta_1$ expression did not vary amongst Control, MR, and MR+βB (Fig. 6). While sGC$\alpha_1$ levels fell slightly in MR+βB compared to either Control or MR, there was no impact on either basal or NO-inducible sGC activity. Baseline and DEA/NO-stimulated cGMP levels were similar for total protein extracts of all hearts.

We again found that caveolae localization protected sGC from oxidation in all hearts. In Cav3$^+$LR, inducible sGC cyclase activity was similar for all study groups (Fig. 5b). Notably, the response to BAY60 was not potentiated within Cav3$^+$LR, relative to control or DEA/NO. In fact, DEA/NO-induced cGMP production exceeded that of BAY60 within Cav3$^+$LR, most significantly for MR and MR+βB, suggesting a predominance of reduced sGC within caveolae. As we previously reported oxidation of sGC within MR NLR, we hypothesized that chronic $\beta_1$-blockade might prevent this stress-induced change in NLR-localized sGC. Indeed, we found that NLR-localized sGC was not oxidized in MR+βB (Fig. 5c). The BAY60 response of MR+βB NLR was markedly blunted compared to that of MR NLR and similar to that of Control NLR.

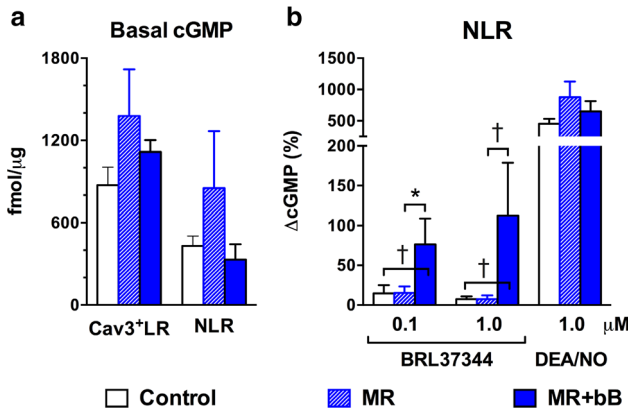


**Fig. 2** Coupling of $\beta_3$AR and NO-sGC-cGMP signaling is detectable within NLR of MR+βB. cGMP levels of Control, MR, and MR+βB Cav3$^+$LR and NLR membrane fractions were measured by EIA at **a** baseline and **b** upon stimulation with selective $\beta_3$AR agonist BRL (0.1 and 1.0 µM) or NO-donor DEA/NO (1.0 µM). No significant BRL response was detected for Cav3$^+$LR in any study group (not shown). All measurements were in the presence of IBMX. Averaged baseline cGMP levels included 10–12 measurements, including replicates, per study group. For summary analysis of BRL stimulated cGMP production, only paired baseline and BRL-induced cGMP levels were included, $n = 4$–6 per study group. For each BRL dose, one-way ANOVA $P \leq 0.1$, $^*P < 0.05$, and $^\dagger P \leq 0.1$ on unpaired student $t$ test. For BRL 0.1 µM dose, Brown-Forsythe $P < 0.05$

## Discussion

We demonstrated that chronic $\beta_1$B in MR is associated with enhanced myocardial NO-sGC-cGMP signaling and $\beta_3$AR/NO-cGMP coupling in specific membrane microdomains. Although myocardial $\beta_3$AR expression was slightly increased, $\beta_3$AR/NO-cGMP coupling could not be detected in untreated MR hearts. Increased oxidation of sGC in MR may have accounted for the lack of $\beta_3$AR/NO-cGMP coupling. In contrast, MR+βB hearts had greater upregulation of myocardial $\beta_3$AR expression, improved sGC redox state, and detectable $\beta_3$AR/NO-cGMP coupling, specifically in heavy-density membrane microdomains. These early changes in myocardial $\beta_3$AR signaling at 4 weeks of metoprolol therapy in MR may contribute to the subsequent potentiated βAR responsiveness and improved cardiac myocyte and LV function seen after more prolonged 4-month metoprolol therapy [43].

Although the functional role of $\beta_3$AR upregulation in HF had been widely debated, several recent studies have clearly shown a cardioprotective role for cardiac $\beta_3$AR signaling. Chronic BRL treatment blunted pathologic cardiac remodeling and improved cardiac function, via a proposed restoration of the nitroso-redox balance, in mice subjected to pressure-overload cardiac stress. [41]. Similarly, transgenic

**Table 2** cGMP levels at baseline and following BRL stimulation within NLR

| | $n$ | Baseline | BRL-stimulated 0.1 µM | BRL-stimulated 1.0 µM |
|---|---|---|---|---|
| Control | 4 | 418.8 ± 166.2 | 438.5 ± 193.3 | 445.9 ± 167.3 |
| MR | 6 | 1,191.0 ± 678.4 | 2,052.0 ± 1,595.0 | 3,345.0 ± 2,965.0 |
| MR+βB | 5 | 503.4 ± 256.8 | 622.3 ± 267.3* | 753.4 ± 314.4$^\dagger$ |

$^* P \leq 0.10$, $^\dagger P < 0.05$ on two-tailed, paired student $t$ test

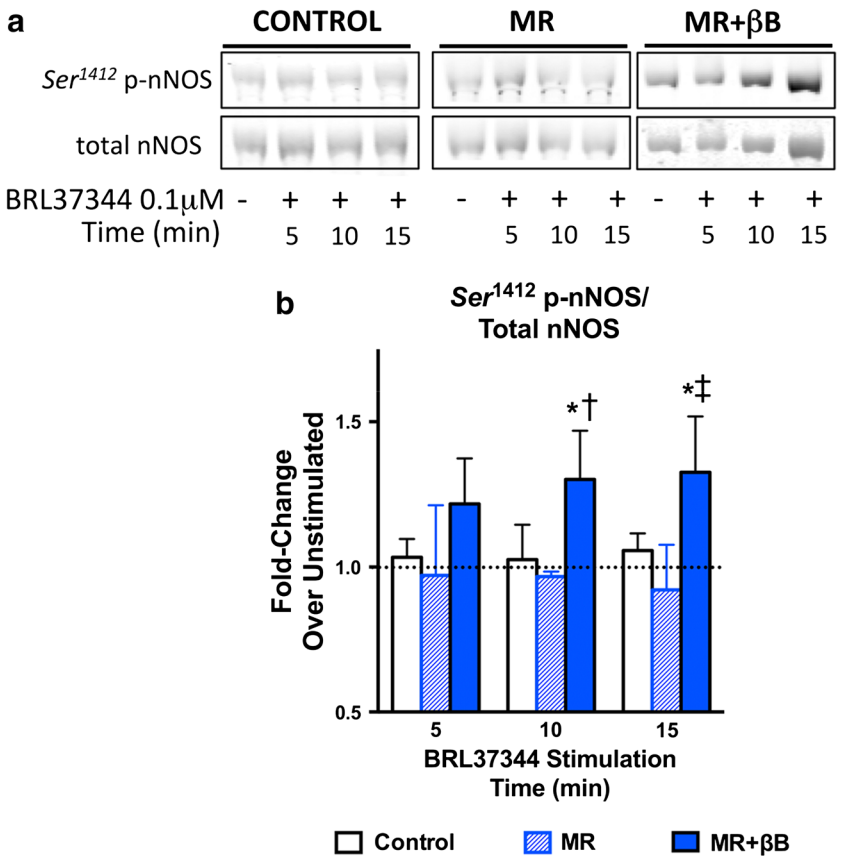


**Fig. 3** Selective $\beta_3$AR agonist BRL induces $Ser^{1412}$-phosphorylation of nNOS within MR+βB NLR. **a** Representative Westerns of $Ser^{1412}$ p-nNOS and total nNOS in Control, MR, and MR+βB NLR. Samples were stimulated with BRL 0.1 μM for 5, 10, and 15 min. **b** Summary densitometry analysis shows the ratio of $Ser^{1412}$ p-nNOS to total nNOS as normalized to unstimulated levels of respective samples, $n = 3$–4 per study group. Two-way ANOVA $P < 0.01$ for study group. Tukey's multiple comparison testing $^{*}P < 0.05$ vs. control, $^{\dagger}P < 0.05$ vs. MR, $^{\ddagger}P < 0.01$ vs. MR

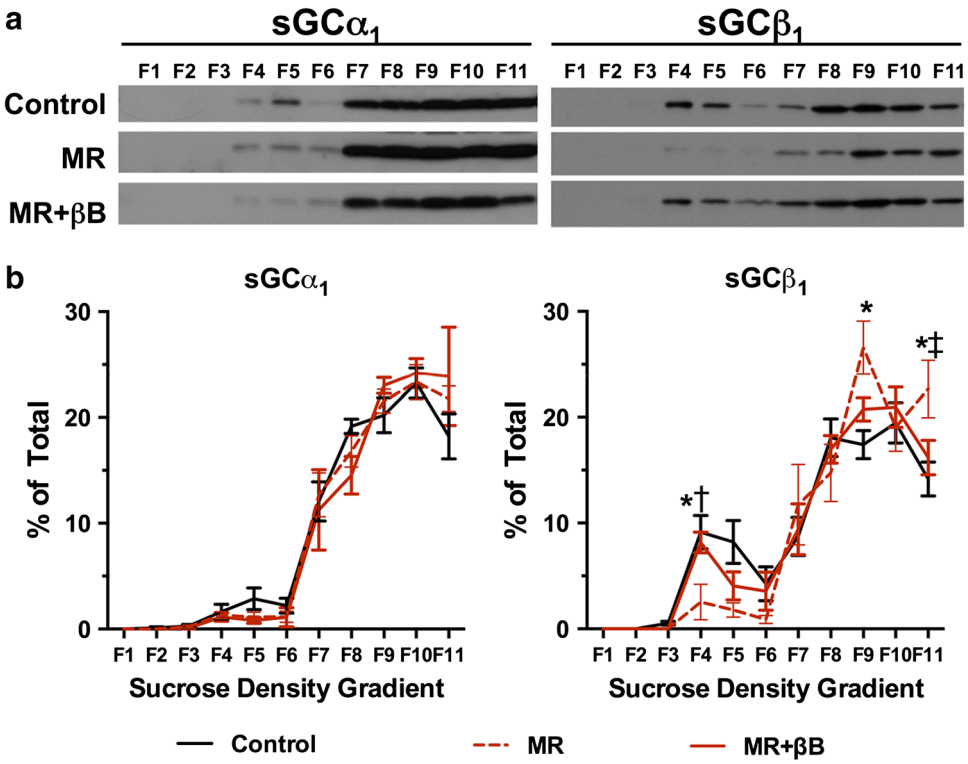


**Fig. 4** sGC$\beta_1$ relocalizes away from caveolae in MR whereas chronic $\beta_1$B therapy preserves Cav3$^{+}$LR localization in MR+βB heart. **a** Representative Westerns of sucrose density gradient fractions of Control, MR, and MR+βB. sGC$\alpha_1$ and sGC$\beta_1$ are enriched in Cav3$^{+}$LR of Control. sGC$\beta_1$ shifts away from F4–F5 in MR, with concomitant relocalization to NLR (F11). sGC$\beta_1$ remains within in Cav3$^{+}$LR in MR+βB. **b** Summary densitometry analysis of all hearts analyzed ($n = 4$–7 per study group). One-way ANOVA for sGC$\beta_1$ $P = 0.012$ for F4, $P = 0.007$ for F9, $P = 0.031$ for F11. Unpaired student $t$ test $^{*}P < 0.05$ for MR vs. control, $^{\dagger}P < 0.05$ for MR+βB vs. MR, $^{\ddagger}P < 0.10$ for MR+βB vs. MR

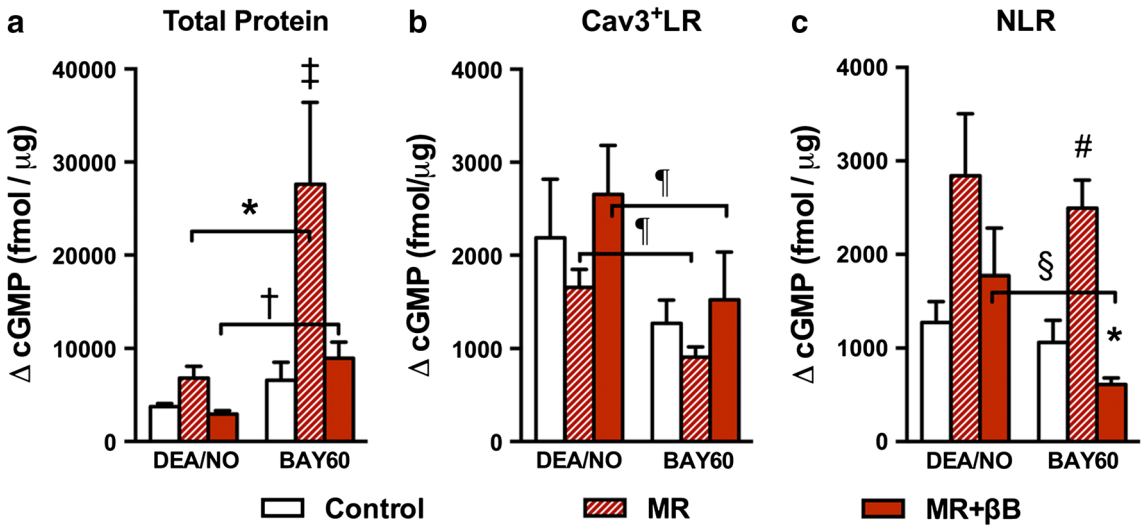


**Fig. 5** Chronic $\beta_1$AR blockade protects sGC from oxidation. **a** BAY60-induced cGMP production markedly exceeds NO-induced cGMP production of MR, indicating predominance of oxidized sGC in MR hearts. Levels of cGMP were measured at baseline and following stimulation with DEA/NO and BAY60 in the presence of IBMX in **a** LV total protein extract, **b** Cav3$^+$LR and **c** NLR fractions. Induced cGMP production is shown as the increment above baseline cGMP levels expressed in fmol cGMP/μg protein. $^*P < 0.01$, $^\dagger P < 0.001$ on ratio paired *t* test; $^\ddagger P < 0.05$ vs. control and MR+βB on Tukey multiple comparison test; $^\P P < 0.1$ on ratio paired *t* test; $^\S P = 0.05$ on ratio paired *t* test; $^\# P < 0.01$ vs. control, $P < 0.001$ vs. MR+βB on Tukey multiple comparison test

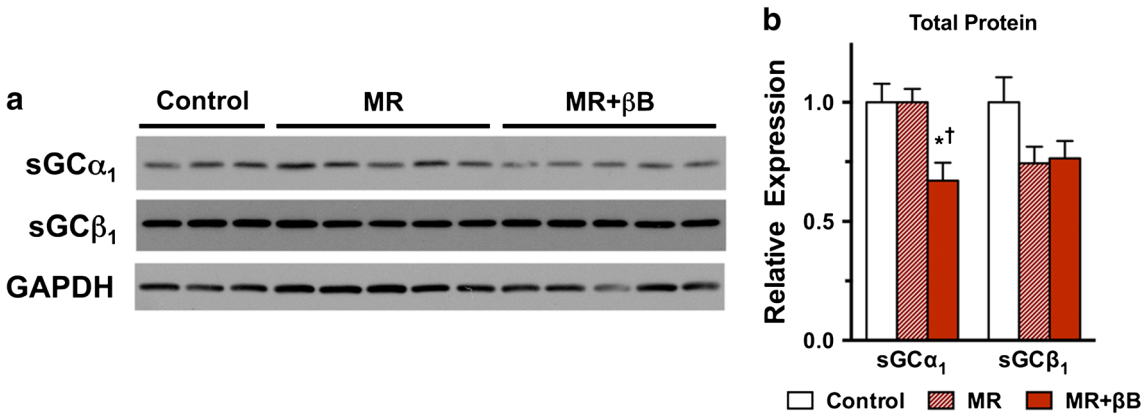


**Fig. 6** Chronic $\beta_1$AR-blockade differentially impacts sGC subunit expression. **a** Representative Western blot of total protein extracts from LV myocardium. **b** Summary densitometry analysis of all Westerns. Signals was standardized to respective GAPDH and then normalized to Control. Mean of replicate measures was used for each heart sample. *Bar graph* represents group mean ± SEM. Total dogs analyzed: Control $n = 6$, MR $n = 5$, and MR+βB $n = 4$. One-way ANOVA $P = 0.007$ for sGC$\alpha_1$; $P = 0.095$ for sGC$\beta_1$

mice with cardiac myocyte-specific expression of human $\beta_3$AR had attenuated hypertrophic response to chronic isoproterenol and angiotensin II stimulation [5]. Cardiac-specific $\beta_3$AR transgenic mice have also been shown to have enhanced cardiac contractility [26]. Furthermore, improved cardiac function and metabolism in a diabetic rat model was associated with metoprolol-induced upregulation of $\beta_3$AR signaling [50, 51].

In the studies reported here, we interrogated a presumed myocardial $\beta_3$AR/NO-cGMP signaling pathway to investigate this as a potential mechanism of cardiac benefit for metoprolol. We previously demonstrated that volume-overload cardiac stress disturbs the nitroso-redox balance as reflected by increased oxidation of sGC in the myocardium [29]. Chronic $\beta_1$AR-blockade not only prevented the nitroso-redox imbalance in volume-overloaded hearts, as reflected by decreased oxidation of sGC in MR+βB hearts, but also induced coupling of $\beta_3$AR and NO-sGC-cGMP signaling in a membrane microdomain specific fashion.

Using the selective $\beta_3$AR agonist BRL, we tested the capacity for $\beta_3$AR triggered cGMP production within LV myocardium, caveolae, and heavy-density, NLR. We compared the BRL response to the DEA/NO response to assess the relative coupling between $\beta_3$AR and NO-sGC-cGMP

signaling. Given reports of caveolae localization of a $\beta_3$AR isoform in mice and of human $\beta_3$AR in a cardiac-specific transgenic mouse [5, 47], along with overall upregulation of $\beta_3$AR in metoprolol-treated diseased hearts [50–52], we expected to find enhanced $\beta_3$AR/NO-cGMP coupling specifically within caveolae of MR+$\beta$B hearts. Strikingly, chronic metoprolol therapy enhanced $\beta_3$AR/NO-cGMP coupling within NLR, not Cav3$^+$LR, of the eccentric hypertrophied heart. In MR hearts, $\beta_3$AR did not increase cGMP production in any myocardial microdomain despite upregulation of $\beta_3$AR. This discrepancy between $\beta_3$AR upregulation and coupling with NO-sGC-cGMP may be explained by the relocalization of sGC$\beta_1$ away from caveolae and the oxidation of sGC within NLR of MR hearts. While the potential signaling partners may be within a shared membrane microdomain, it appears that inducible sGC cyclase activity was compromised by oxidation.

Alternatively, coupling of $\beta_3$AR and NO-sGC-cGMP within MR+$\beta$B NLR might reflect local coupling of $\beta_3$AR and nNOS. Recent studies in rodents demonstrated that $\beta_3$AR signaling activates nNOS, as the effects of $\beta_3$AR-mediated cardioprotection, NO production, and NOS signaling were blunted in mice with genetically deleted nNOS [41]. Moreover, $\beta_3$AR activation of nNOS was found to occur via phosphorylation of the nNOS positive regulatory site, $Ser^{1412}$ [5, 41, 60]. While levels of $Ser^{1412}$–phosphorylated nNOS (p-nNOS) are low under physiological conditions, nNOS activation, as reflected by elevated $Ser^{1412}$ p-nNOS, may play a critical counter-regulatory role in stress induced, pathophysiological conditions. In our canine model, selective $\beta_3$AR agonist BRL induced an increase in $Ser^{1412}$ p-nNOS within NLR of MR+$\beta$B but not in MR or Control, which is consistent with our findings of BRL-induced cGMP production within NLR of MR+$\beta$B alone. These findings as a whole suggest that $\beta_1$AR-blockade within the volume-overloaded heart induces $\beta_3$AR/NO-cGMP coupling via enhanced $\beta_3$AR activation of nNOS.

Our findings regarding $\beta_3$AR and NO-sGC-cGMP signaling are novel and significant on several fronts. We are the first to demonstrate active and inducible coupling of $\beta_3$AR and NO-sGC-cGMP signaling within the heart, notably in the $\beta_1$B-treated, volume-overloaded heart and in a microdomain specific fashion. Recent studies of a double transgenic mouse with cardiac myocyte-specific expression of both the human $\beta_3$AR and a cGMP-specific FRET sensor revealed increased basal sGC activity [5]. However, inducible or active coupling between $\beta_3$AR and NO-sGC-cGMP was not interrogated. Our findings suggest that chronic $\beta_1$B therapy is associated with a beneficial inducible and active $\beta_3$AR/NO-cGMP coupling outside of myocardial caveolae. This is consistent with reports of (a) differential subcellular localization and G protein coupling of murine $\beta_3$AR isoforms [47]; and (b) $G_i$ mediation of GPCR activation of NOS [3, 10]. Moreover, previously reported nuclear $\beta_3$AR regulation of gene transcription depends upon local downstream NO-sGC-cGMP activation [58]. While more studies are warranted to elucidate the mechanistic details, such reports of nuclear $\beta_3$AR activation of NO-sGC-cGMP signaling raise the possibility that the NLR microdomain may encompass nuclear envelope.

Interestingly, chronic metoprolol treatment was associated with the retention of sGC$\beta_1$ within caveolae. As the exact mechanism of caveolae localization of sGC$\beta_1$ remains to be determined, we can only hypothesize at this time that chronic $\beta_1$AR-blockade either directly or indirectly impacts upon protein–protein interactions or reversible post-translational modifications (e.g. *S*-palmitoylation) that are generally believed to mediate caveolae localization [11, 22, 63]. Such studies are beyond the scope of this manuscript.

Myocardial $\beta_3$AR expression is challenging to assess given the low expression of $\beta_3$AR relative to $\beta_1$AR and $\beta_2$AR in the heart [36]. While radioligand binding assays are commonly used to determine receptor expression, high-affinity and high-specificity radiolabeled $\beta$AR subtype antagonists are necessary to differentiate the relative expression of the three $\beta$AR subtypes. In adipose tissue, which predominantly expresses $\beta_3$ AR over either $\beta_1$AR or $\beta_2$AR, radioligand binding assays are feasible for determining $\beta_3$AR expression. However, the lack of high-affinity, selective $\beta_3$AR antagonists precludes the use of radioligand binding assays for determining $\beta_3$AR expression and distribution in the heart [12, 37, 39]. The exceedingly high concentration of radioligand $\beta_3$AR antagonist needed would lead to high non-specific binding and inaccurate characterization of $\beta_3$AR expression. Hence, in lieu of radioligand binding assay, we selected a highly sensitive and specific $\beta_3$AR antibody that recognizes an epitope conserved within both canine and human $\beta_3$AR amino acid sequences and has only 60–80 % identity, at high E values, with $\beta_1$AR or $\beta_2$AR amino acid sequences. We confirmed our Western analysis with qRT-PCR. Most importantly, we successfully demonstrated functional coupling of $\beta_3$AR/NO-cGMP signaling with our in vitro BRL stimulation studies.

Our assessment of myocardial microdomain signaling is, by necessity, synthetic in nature, in that cyclase activity assays are performed on myocardial membrane fractions, as opposed to live, intact cardiac myocytes. Ideally, subcellular cGMP signaling within caveolae- and heavy-density NLR microdomains could be visualized in live cells with a FRET-based cGMP sensor. While transgenic mice with cardiac myocyte-specific expression of FRET-based cGMP sensors have recently been reported [5, 56], none

are microdomain-targeted cGMP sensors. Thus, our combinatorial approach of cGMP enzyme immunoassays and Western analyses effectively allow us to interrogate microdomain signaling.

This study shows for the first time that chronic $\beta_1$B with metoprolol therapy preserves and even enhances NO-cGMP signaling within specific myocardial microdomains in the volume-overloaded heart, in particular inducing coupling of $\beta_3$AR/NO-cGMP signaling in the heavy-density non-lipid raft fraction. The present analysis raises the possibility that the antioxidant action shared by βBs may be an indirect restoration of nitroso-redox balance in myocardial NLR membrane microdomain, mediated by enhanced $\beta_3$AR signaling coupled with nNOS activation and sGC stimulation (Fig. 7). This indirect antioxidant mechanism may be particular to selective $\beta_1$-blockers, or even metoprolol succinate for that matter. Whereas metoprolol upregulates myocardial $\beta_3$AR expression, the non-selective β-blocker carvedilol does not [64]. Whereas carvedilol can directly scavenge free radicals, selective $\beta_1$-blockers do not [54]. In fact, carvedilol has been shown to block oxidative stress-mediated signaling via various mechanisms [27]. Thus, the comparative cardioprotection and cardioprotective mechanism of $\beta_1$B metoprolol versus non-selective βBs may depend upon the etiology of HF and thereby the effect of the specific cardiac injury upon myocardial NO and/or $\beta_3$AR signaling [28]. Regardless, the enhancement of myocardial $\beta_3$AR/NO-cGMP coupling with chronic $\beta_1$AR-blockade in the volume-overloaded heart suggests new approaches to βAR modulation to optimize cardiac function. βAR modulation, with initial chronic $\beta_1$AR antagonism followed by additional $\beta_3$AR agonism, may offer further functional and clinical benefit to HF and MR patients. Moreover, direct stimulation of myocardial sGC on a background of neurohormonal blockade may similarly confer additional clinical benefit [13]. Such potential therapeutic implications warrant further mechanistic and eventual clinical studies.

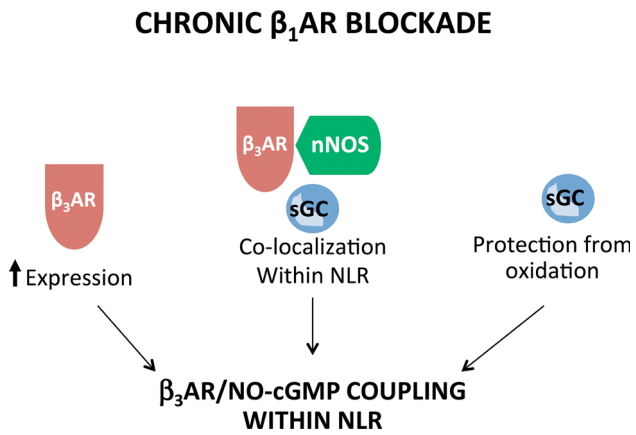


**Fig. 7** $\beta_1$AR-blockade enhances coupling of $\beta_3$AR and NO-sGC-cGMP signaling within myocardial NLR. Increased myocardial $\beta_3$AR expression, colocalization of $\beta_3$AR, sGC, and nNOS, and protection of sGC from oxidation contribute to the enhanced $\beta_3$AR/NO-cGMP coupling in chronic $\beta_1$B treated, volume-overloaded hearts

**Acknowledgments** We thank K. Joseph Hurt for providing the p-nNOS antibody; Johannes-Peter Stasch for providing BAY 60-2770; and Doug Tilley for reviewing the manuscript. This research was supported by the American Heart Association (Post-Doctoral Fellowship to D.M. Trappanese, Scientist Development Grant to E.J. Tsai), NIH (T32-HL091804 to S.R. Houser; R37-HL061690, R01-HL085503, P01-HL075443, and P01-HL108806 to W.J. Koch; P01-HL74237 and R01-HL108213 to F.A. Recchia; P50-HL077100 to L. Dell'Italia; K08-HL109159 to E.J. Tsai), and the Pennsylvania Department of Health (E.J. Tsai).

**Conflict of interest** On behalf of all the authors, the corresponding author states that there is no conflict of interest.

## References

1. Aragon JP, Condit ME, Bhushan S, Predmore BL, Patel SS, Grinsfelder DB, Gundewar S, Jha S, Calvert JW, Barouch LA, Lavu M, Wright HM, Lefer DJ (2011) Beta3-adrenoreceptor stimulation ameliorates myocardial ischemia-reperfusion injury via endothelial nitric oxide synthase and neuronal nitric oxide synthase activation. J Am Coll Cardiol 58:2683–2691. doi:10.1016/j.jacc.2011.09.033
2. Balijepalli RC, Foell JD, Hall DD, Hell JW, Kamp TJ (2006) Localization of cardiac L-type Ca(2+) channels to a caveolar macromolecular signaling complex is required for beta(2)-adrenergic regulation. Proc Natl Acad Sci USA 103:7500–7505
3. Banquet S, Delannoy E, Agouni A, Dessy C, Lacomme S, Hubert F, Richard V, Muller B, Leblais V (2011) Role of G(i/o)-Src kinase-PI3K/Akt pathway and caveolin-1 in beta(2)-adrenoceptor coupling to endothelial NO synthase in mouse pulmonary artery. Cell Signal 23:1136–1143. doi:10.1016/j.cellsig.2011.02.008
4. Bartholomeu JB, Vanzelli AS, Rolim NP, Ferreira JC, Bechara LR, Tanaka LY, Rosa KT, Alves MM, Medeiros A, Mattos KC, Coelho MA, Irigoyen MC, Krieger EM, Krieger JE, Negrao CE, Ramires PR, Guatimosim S, Brum PC (2008) Intracellular mechanisms of specific beta-adrenoceptor antagonists involved in improved cardiac function and survival in a genetic model of heart failure. J Mol Cell Cardiol 45:240–249. doi:10.1016/j.yjmcc.2008.05.011
5. Belge C, Hammond J, Dubois-Deruy E, Manoury B, Hamelet J, Beauloye C, Markl A, Pouleur AC, Bertrand L, Esfahani H, Jnaoui K, Gotz KR, Nikolaev VO, Vanderper A, Herijgers P, Lobysheva I, Iaccarino G, Hilfiker-Kleiner D, Tavernier G, Langin D, Dessy C, Balligand JL (2013) Enhanced expression of beta3-adrenoceptors in cardiac myocytes attenuates neurohormone-induced hypertrophic remodeling through nitric oxide synthase. Circulation 129:451–462. doi:10.1161/CIRCULATIONAHA.113.004940
6. Bohm M, Deutsch HJ, Hartmann D, Rosee KL, Stablein A (1997) Improvement of postreceptor events by metoprolol treatment in patients with chronic heart failure. J Am Coll Cardiol 30:992–996
7. Bundgaard H, Liu CC, Garcia A, Hamilton EJ, Huang Y, Chia KK, Hunyor SN, Figtree GA, Rasmussen HH (2010) beta(3) adrenergic stimulation of the cardiac Na+-K+ pump by reversal

of an inhibitory oxidative modification. Circulation 122:2699–2708. doi:10.1161/CIRCULATIONAHA.110.964619
8. Cheng HJ, Zhang ZS, Onishi K, Ukai T, Sane DC, Cheng CP (2001) Upregulation of functional beta(3)-adrenergic receptor in the failing canine myocardium. Circ Res 89:599–606
9. Damy T, Ratajczak P, Shah AM, Camors E, Marty I, Hasenfuss G, Marotte F, Samuel JL, Heymes C (2004) Increased neuronal nitric oxide synthase-derived NO production in the failing human heart. Lancet 363:1365–1367. doi:10.1016/S0140-6736(04)16048-0
10. Datar R, Kaesemeyer WH, Chandra S, Fulton DJ, Caldwell RW (2010) Acute activation of eNOS by statins involves scavenger receptor-B1, G protein subunit Gi, phospholipase C and calcium influx. Br J Pharmacol 160:1765–1772. doi:10.1111/j.1476-5381.2010.00817.x
11. Feron O, Michel JB, Sase K, Michel T (1998) Dynamic regulation of endothelial nitric oxide synthase: complementary roles of dual acylation and caveolin interactions. Biochemistry 37:193–200. doi:10.1021/bi972307p
12. Feve B, Emorine LJ, Lasnier F, Blin N, Baude B, Nahmias C, Strosberg AD, Pairault J (1991) Atypical beta-adrenergic receptor in 3T3-F442A adipocytes. Pharmacological and molecular relationship with the human beta 3-adrenergic receptor. J Biol Chem 266:20329–20336
13. Fraccarollo D, Galuppo P, Schmidt I, Ertl G, Bauersachs J (2005) Additive amelioration of left ventricular remodeling and molecular alterations by combined aldosterone and angiotensin receptor blockade after myocardial infarction. Cardiovasc Res 67:97–105. doi:10.1016/j.cardiores.2005.03.001
14. Garcia-Prieto J, Garcia-Ruiz JM, Sanz-Rosa D, Pun A, Garcia-Alvarez A, Davidson SM, Fernandez-Friera L, Nuno-Ayala M, Fernandez-Jimenez R, Bernal JA, Izquierdo-Garcia JL, Jimenez-Borreguero J, Pizarro G, Ruiz-Cabello J, Macaya C, Fuster V, Yellon DM, Ibanez B (2014) beta3 adrenergic receptor selective stimulation during ischemia/reperfusion improves cardiac function in translational models through inhibition of mPTP opening in cardiomyocytes. Basic Res Cardiol 109:422. doi:10.1007/s00395-014-0422-0
15. Gauthier C, Leblais V, Kobzik L, Trochu JN, Khandoudi N, Bril A, Balligand JL, Le Marec H (1998) The negative inotropic effect of beta3-adrenoceptor stimulation is mediated by activation of a nitric oxide synthase pathway in human ventricle. J Clin Invest 102:1377–1384. doi:10.1172/JCI2191
16. George I, Sabbah HN, Xu K, Wang N, Wang J (2011) beta-adrenergic receptor blockade reduces endoplasmic reticulum stress and normalizes calcium handling in a coronary embolization model of heart failure in canines. Cardiovasc Res 91:447–455. doi:10.1093/cvr/cvr106
17. Hankes GH, Ardell JL, Tallaj J, Wei CC, Aban I, Holland M, Rynders P, Dillon R, Cardinal R, Hoover DB, Armour JA, Husain A, Dell'Italia LJ (2006) Beta1-adrenoceptor blockade mitigates excessive norepinephrine release into cardiac interstitium in mitral regurgitation in dog. Am J Physiol Heart Circ Physiol 291:H147–H151. doi:10.1152/ajpheart.00951.2005
18. Heilbrunn SM, Shah P, Bristow MR, Valantine HA, Ginsburg R, Fowler MB (1989) Increased beta-receptor density and improved hemodynamic response to catecholamine stimulation during long-term metoprolol therapy in heart failure from dilated cardiomyopathy. Circulation 79:483–490. doi:10.1161/01.CIR.79.3.483
19. Heusch G (2011) Beta3-adrenoceptor activation just says NO to myocardial reperfusion injury. J Am Coll Cardiol 58:2692–2694. doi:10.1016/j.jacc.2011.09.034
20. Hurt KJ, Sezen SF, Lagoda GF, Musicki B, Rameau GA, Snyder SH, Burnett AL (2012) Cyclic AMP-dependent phosphorylation of neuronal nitric oxide synthase mediates penile erection. Proc Natl Acad Sci USA 109:16624–16629. doi:10.1073/Pnas.1213790109
21. Iaccarino G, Tomhave ED, Lefkowitz RJ, Koch WJ (1998) Reciprocal in vivo regulation of myocardial G protein-coupled receptor kinase expression by beta-adrenergic receptor stimulation and blockade. Circulation 98:1783–1789. doi:10.1161/01.CIR.98.17.1783
22. Ishizaka N, Griendling KK, Lassegue B, Alexander RW (1998) Angiotensin II type 1 receptor: relationship with caveolae and caveolin after initial agonist stimulation. Hypertension 32:459–466
23. Iwakiri Y, Satoh A, Chatterjee S, Toomre DK, Chalouni CM, Fulton D, Groszmann RJ, Shah VH, Sessa WC (2006) Nitric oxide synthase generates nitric oxide locally to regulate compartmentalized protein S-nitrosylation and protein trafficking. Proc Natl Acad Sci USA 103:19777–19782. doi:10.1073/pnas.0605907103
24. Jones AW, Durante W, Korthuis RJ (2010) Heme oxygenase-1 deficiency leads to alteration of soluble guanylate cyclase redox regulation. J Pharmacol Exp Ther 335:85–91. doi:10.1124/jpet.110.169755
25. Kleaveland JP, Kussmaul WG, Vinciguerra T, Diters R, Carabello BA (1988) Volume overload hypertrophy in a closed-chest model of mitral regurgitation. Am J Physiol 254:H1034–H1041
26. Kohout TA, Takaoka H, McDonald PH, Perry SJ, Mao L, Lefkowitz RJ, Rockman HA (2001) Augmentation of cardiac contractility mediated by the human beta(3)-adrenergic receptor overexpressed in the hearts of transgenic mice. Circulation 104:2485–2491
27. Koitabashi N, Arai M, Tomaru K, Takizawa T, Watanabe A, Niwano K, Yokoyama T, Wuytack F, Periasamy M, Nagai R, Kurabayashi M (2005) Carvedilol effectively blocks oxidative stress-mediated downregulation of sarcoplasmic reticulum Ca2+-ATPase 2 gene transcription through modification of Sp1 binding. Biochem Biophys Res Commun 328:116–124. doi:10.1016/j.bbrc.2004.12.139
28. Le DE, Pascotto M, Leong-Poi H, Sari I, Micari A, Kaul S (2013) Anti-inflammatory and pro-angiogenic effects of beta blockers in a canine model of chronic ischemic cardiomyopathy: comparison between carvedilol and metoprolol. Basic Res Cardiol 108:384. doi:10.1007/s00395-013-0384-7
29. Liu Y, Dillon AR, Tillson M, Makarewich C, Nguyen V, Dell'Italia L, Sabri AK, Rizzo V, Tsai EJ (2013) Volume overload induces differential spatiotemporal regulation of myocardial soluble guanylyl cyclase in eccentric hypertrophy and heart failure. J Mol Cell Cardiol 60:72–83. doi:10.1016/j.yjmcc.2013.03.019
30. Macdougall DA, Agarwal SR, Stopford EA, Chu H, Collins JA, Longster AL, Colyer J, Harvey RD, Calaghan S (2012) Caveolae compartmentalise beta2-adrenoceptor signals by curtailing cAMP production and maintaining phosphatase activity in the sarcoplasmic reticulum of the adult ventricular myocyte. J Mol Cell Cardiol 52:388–400. doi:10.1016/j.yjmcc.2011.06.014
31. Maczewski M, Mackiewicz U (2008) Effect of metoprolol and ivabradine on left ventricular remodelling and Ca2+ handling in the post-infarction rat heart. Cardiovasc Res 79:42–51. doi:10.1093/cvr/cvn057
32. Makarewich CA, Correll RN, Gao H, Zhang H, Yang B, Berretta RM, Rizzo V, Molkentin JD, Houser SR (2012) A caveolae-targeted L-type Ca(2)+ channel antagonist inhibits hypertrophic signaling without reducing cardiac contractility. Circ Res 110:669–674. doi:10.1161/CIRCRESAHA.111.264028
33. Markandeya YS, Fahey JM, Pluteanu F, Cribbs LL, Balijepalli RC (2011) Caveolin-3 regulates protein kinase A modulation of the Ca(V)3.2 (alpha1H) T-type Ca2+ channels. J Biol Chem 286:2433–2444. doi:10.1074/jbc.M110.182550

34. Mehta RH, Supiano MA, Oral H, Grossman PM, Montgomery DS, Smith MJ, Starling MR (2003) Compared with control subjects, the systemic sympathetic nervous system is activated in patients with mitral regurgitation. Am Heart J 145:1078–1085. doi:10.1016/S0002-8703(03)00111-X
35. Moniotte S, Kobzik L, Feron O, Trochu JN, Gauthier C, Balligand JL (2001) Upregulation of beta(3)-adrenoceptors and altered contractile response to inotropic amines in human failing myocardium. Circulation 103:1649–1655
36. Monto F, Oliver E, Vicente D, Rueda J, Aguero J, Almenar L, Ivorra MD, Barettino D, D'Ocon P (2012) Different expression of adrenoceptors and GRKs in the human myocardium depends on heart failure etiology and correlates to clinical variables. Am J Physiol Heart Circ Physiol 303:H368–H376. doi:10.1152/ajpheart.01061.2011
37. Muzzin P, Revelli JP, Fraser CM, Giacobino JP (1992) Radioligand binding studies of the atypical beta 3-adrenergic receptor in rat brown adipose tissue using [3H]CGP 12177. FEBS Lett 298:162–164. doi:10.1016/0014-5793(92)80046-J
38. Nagatomo Y, Yoshikawa T, Kohno T, Yoshizawa A, Anzai T, Meguro T, Satoh T, Ogawa S (2007) Effects of beta-blocker therapy on high sensitivity c-reactive protein, oxidative stress, and cardiac function in patients with congestive heart failure. J Card Fail 13:365–371. doi:10.1016/j.cardfail.2007.02.004
39. Nahmias C, Blin N, Elalouf JM, Mattei MG, Strosberg AD, Emorine LJ (1991) Molecular characterization of the mouse beta 3-adrenergic receptor: relationship with the atypical receptor of adipocytes. EMBO J 10:3721–3727
40. Napp A, Brixius K, Pott C, Ziskoven C, Boelck B, Mehlhorn U, Schwinger RH, Bloch W (2009) Effects of the beta3-adrenergic agonist BRL 37344 on endothelial nitric oxide synthase phosphorylation and force of contraction in human failing myocardium. J Card Fail 15:57–67. doi:10.1016/j.cardfail.2008.08.006
41. Niu X, Watts VL, Cingolani OH, Sivakumaran V, Leyton-Mange JS, Ellis CL, Miller KL, Vandegaer K, Bedja D, Gabrielson KL, Paolocci N, Kass DA, Barouch LA (2012) Cardioprotective effect of beta-3 adrenergic receptor agonism: role of neuronal nitric oxide synthase. J Am Coll Cardiol 59:1979–1987. doi:10.1016/j.jacc.2011.12.046
42. Oh P, Schnitzer JE (1999) Immunoisolation of caveolae with high affinity antibody binding to the oligomeric caveolin cage. Toward understanding the basis of purification. J Biol Chem 274:23144–23154. doi:10.1074/jbc.274.33.23144
43. Pat B, Killingsworth C, Denney T, Zheng J, Powell P, Tillson M, Dillon AR, Dell'Italia LJ (2008) Dissociation between cardiomyocyte function and remodeling with beta-adrenergic receptor blockade in isolated canine mitral regurgitation. Am J Physiol Heart Circ Physiol 295:H2321–H2327. doi:10.1152/ajpheart.00746.2008
44. Rizzo V, Morton C, DePaola N, Schnitzer JE, Davies PF (2003) Recruitment of endothelial caveolae into mechanotransduction pathways by flow conditioning in vitro. Am J Physiol Heart Circ Physiol 285:H1720–H1729. doi:10.1152/ajpheart.00344.2002
45. Rybin VO, Xu X, Lisanti MP, Steinberg SF (2000) Differential targeting of beta -adrenergic receptor subtypes and adenylyl cyclase to cardiomyocyte caveolae. A mechanism to functionally regulate the cAMP signaling pathway. J Biol Chem 275:41447–41457
46. Sabri A, Rafiq K, Seqqat R, Kolpakov MA, Dillon R, Dell'italia LJ (2008) Sympathetic activation causes focal adhesion signaling alteration in early compensated volume overload attributable to isolated mitral regurgitation in the dog. Circ Res 102:1127–1136
47. Sato M, Hutchinson DS, Halls ML, Furness SG, Bengtsson T, Evans BA, Summers RJ (2012) Interaction with caveolin-1 modulates G protein coupling of mouse beta3-adrenoceptor. J Biol Chem 287:20674–20688. doi:10.1074/jbc.M111.280651
48. Schmidt K, Neubauer A, Kolesnik B, Stasch JP, Werner ER, Gorren AC, Mayer B (2012) Tetrahydrobiopterin protects soluble guanylate cyclase against oxidative inactivation. Mol Pharmacol 82:420–427. doi:10.1124/mol.112.079855
49. Schwencke C, Okumura S, Yamamoto M, Geng YJ, Ishikawa Y (1999) Colocalization of beta-adrenergic receptors and caveolin within the plasma membrane. J Cell Biochem 75:64–72
50. Sharma V, Dhillon P, Wambolt R, Parsons H, Brownsey R, Allard MF, McNeill JH (2008) Metoprolol improves cardiac function and modulates cardiac metabolism in the streptozotocin-diabetic rat. Am J Physiol Heart Circ Physiol 294:H1609–H1620. doi:10.1152/ajpheart.00949.2007
51. Sharma V, Parsons H, Allard MF, McNeill JH (2008) Metoprolol increases the expression of beta(3)-adrenoceptors in the diabetic heart: effects on nitric oxide signaling and forkhead transcription factor-3. Eur J Pharmacol 595:44–51. doi:10.1016/j.ejphar.2008.07.042
52. Sharma V, Sharma A, Saran V, Bernatchez PN, Allard MF, McNeill JH (2011) beta-receptor antagonist treatment prevents activation of cell death signaling in the diabetic heart independent of its metabolic actions. Eur J Pharmacol 657:117–125. doi:10.1016/j.ejphar.2011.01.044
53. Spoladore R, Fragasso G, Perseghin G, De Cobelli F, Esposito A, Maranta F, Calori G, Locatelli M, Lattuada G, Scifo P, Del Maschio A, Margonato A (2013) Beneficial effects of beta-blockers on left ventricular function and cellular energy reserve in patients with heart failure. Fundam Clin Pharmacol 27:455–464. doi:10.1111/j.1472-8206.2012.01029.x
54. Szajerski P, Zielonka J, Sikora A, Adamus J, Marcinek A, Gebicki J, Kozlovski VI, Drelicharz L, Chlopicki S (2006) Radical scavenging and NO-releasing properties of selected beta-adrenoreceptor antagonists. Free Radic Res 40:741–752
55. Takimoto E, Champion HC, Belardi D, Moslehi J, Mongillo M, Mergia E, Montrose DC, Isoda T, Aufiero K, Zaccolo M, Dostmann WR, Smith CJ, Kass DA (2005) cGMP catabolism by phosphodiesterase 5A regulates cardiac adrenergic stimulation by NOS3-dependent mechanism. Circ Res 96:100–109. doi:10.1161/01.RES.0000152262.22968.72
56. Thunemann M, Wen L, Hillenbrand M, Vachaviolos A, Feil S, Ott T, Han X, Fukumura D, Jain RK, Russwurm M, de Wit C, Feil R (2013) Transgenic mice for cGMP imaging. Circ Res 113:365–371. doi:10.1161/CIRCRESAHA.113.301063
57. Tsai EJ, Liu Y, Koitabashi N, Bedja D, Danner T, Jasmin JF, Lisanti MP, Friebe A, Takimoto E, Kass DA (2012) Pressure-overload-induced subcellular relocalization/oxidation of soluble guanylyl cyclase in the heart modulates enzyme stimulation. Circ Res 110:295–303
58. Vaniotis G, Glazkova I, Merlen C, Smith C, Villeneuve LR, Chatenet D, Therien M, Fournier A, Tadevosyan A, Trieu P, Nattel S, Hebert TE, Allen BG (2013) Regulation of cardiac nitric oxide signaling by nuclear beta-adrenergic and endothelin receptors. J Mol Cell Cardiol 62:58–68. doi:10.1016/j.yjmcc.2013.05.003
59. Waagstein F, Caidahl K, Wallentin I, Bergh CH, Hjalmarson A (1989) Long-term beta-blockade in dilated cardiomyopathy. Effects of short- and long-term metoprolol treatment followed by withdrawal and readministration of metoprolol. Circulation 80:551–563. doi:10.1161/01.CIR.80.3.551
60. Watts VL, Sepulveda FM, Cingolani OH, Ho AS, Niu X, Kim R, Miller KL, Vandegaer K, Bedja D, Gabrielson KL, Rameau G, O'Rourke B, Kass DA, Barouch LA (2013) Anti-hypertrophic and anti-oxidant effect of beta3-adrenergic stimulation in myocytes requires differential neuronal NOS phosphorylation. J Mol Cell Cardiol 62:8–17. doi:10.1016/j.yjmcc.2013.04.025
61. Whalen EJ, Foster MW, Matsumoto A, Ozawa K, Violin JD, Que LG, Nelson CD, Benhar M, Keys JR, Rockman HA, Koch WJ,

Daaka Y, Lefkowitz RJ, Stamler JS (2007) Regulation of beta-adrenergic receptor signaling by S-nitrosylation of G-protein-coupled receptor kinase 2. Cell 129:511–522. doi:10.1016/j.cell.2007.02.046

62. Wu JL, Liu WZ, Liu JH, Qiao LY, Yuan YN (2011) Distribution and quantification of beta-3 adrenergic receptor in tissues of sheep. Animal 5:88–93. doi:10.1017/S1751731110001564
63. Yeh DC, Duncan JA, Yamashita S, Michel T (1999) Depalmitoylation of endothelial nitric-oxide synthase by acyl-protein thioesterase 1 is potentiated by Ca(2+)-calmodulin. J Biol Chem 274:33148–33154
64. Zhao Q, Wu TG, Jiang ZF, Chen GW, Lin Y, Wang LX (2007) Effect of beta-blockers on beta3-adrenoceptor expression in chronic heart failure. Cardiovasc Drugs Ther 21:85–90. doi:10.1007/s10557-007-6016-4
65. Zhao Q, Zeng F, Liu JB, He Y, Li B, Jiang ZF, Wu TG, Wang LX (2013) Upregulation of beta3-adrenergic receptor expression in the atrium of rats with chronic heart failure. J Cardiovasc Pharmacol Ther 18:133–137. doi:10.1177/1074248412460123
66. Zheng J, Yancey DM, Ahmed MI, Wei CC, Powell PC, Shanmugam M, Gupta H, Lloyd SG, McGiffin DC, Schiros CG, Denney TS Jr, Babu GJ, Dell'italia LJ (2014) Increased sarcolipin expression and adrenergic drive in humans with preserved left ventricular ejection fraction and chronic isolated mitral regurgitation. Circ Heart Fail 7:194–202. doi:10.1161/CIRCHEARTFAILURE.113.000519